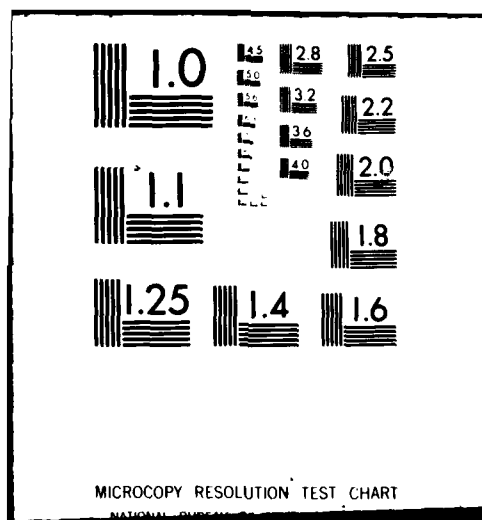


AD-A116 261 ARIZONA UNIV TUCSON ENGINEERING EXPERIMENT STATION F/8 1/3  
SHOCK-FREE CONFIGURATIONS IN TWO- AND THREE- DIMENSIONAL TRANSO-ETC(U)  
MAY 81 A R SEEBASS N00014-76-C-0182  
UNCLASSIFIED NL  
TFD-81-04

1  
2  
3  
4  
5

END  
DATE  
7-82  
FILED  
DTIC



DTIC

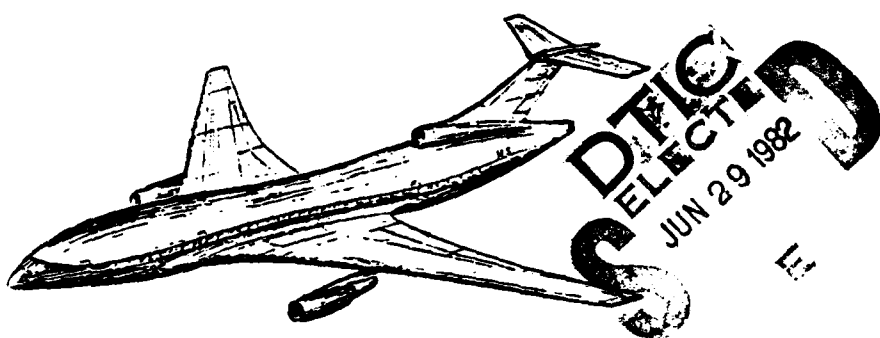
TRANSONIC FLUID DYNAMICS

①

Report TFD 81-04

R. Seebass

SHOCK-FREE CONFIGURATIONS IN  
TWO- AND THREE- DIMENSIONAL TRANSONIC FLOW



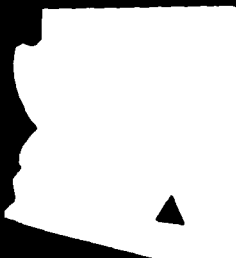
Naval Research Lab.

SEP 24 1981

May 1981

Naval Research Laboratory

AD A116261



This document has been approved  
for public release and sale; its  
distribution is unlimited.

**ENGINEERING EXPERIMENT STATION  
COLLEGE OF ENGINEERING**

THE UNIVERSITY OF ARIZONA  
TUCSON, ARIZONA 85721

DTIC FILE COPY  
82 08 10 077

SECURITY CLASSIFICATION OF THIS PAGE (When Data Entered)

REPORT DOCUMENTATION PAGE		READ INSTRUCTIONS BEFORE COMPLETING FORM
1. REPORT NUMBER	2. GOVT ACCESSION NO.	3. RECIPIENT'S CATALOG NUMBER
		<i>AD-A116 261</i>
4. TITLE (and Subtitle)  SHOCK-FREE CONFIGURATIONS IN TWO- AND THREE- DIMENSIONAL TRANSONIC FLOW		5. TYPE OF REPORT & PERIOD COVERED
7. AUTHOR(s)  A. R. Seebass		6. PERFORMING ORG. REPORT NUMBER  TFD 81-04
9. PERFORMING ORGANIZATION NAME AND ADDRESS  University of Arizona Aerospace and Mechanical Engineering Tucson, Arizona 85720		8. CONTRACT OR GRANT NUMBER(s)  N00014-76-C-0182
11. CONTROLLING OFFICE NAME AND ADDRESS  Office of Naval Research (code 438) Arlington, Virginia 22217		10. PROGRAM ELEMENT, PROJECT, TASK AREA & WORK UNIT NUMBERS
14. MONITORING AGENCY NAME & ADDRESS (if different from Controlling Office)  Office of Naval Research Resident Representative Room 223 Bandelier Hall West University of New Mexico Albuquerque, NM 87131		12. REPORT DATE  May 1981
		13. NUMBER OF PAGES  20
		15. SECURITY CLASS. (of this report)  Unclassified
		15a. DECLASSIFICATION/DOWNGRADING SCHEDULE
16. DISTRIBUTION STATEMENT (of this Report)  Approved for Public Release: distribution unlimited.		
17. DISTRIBUTION STATEMENT (of the abstract entered in Block 20, if different from Report)		
18. SUPPLEMENTARY NOTES		
19. KEY WORDS (Continue on reverse side if necessary and identify by block number)  Shock-free Design Airfoil Design Wing Design		
20. ABSTRACT (Continue on reverse side if necessary and identify by block number)  An indirect method for finding shock-free airfoils and a nearly direct method for finding shock-free airfoils and wing are discussed. While the mathematics of both procedures is emphasized, illustrative practical results are given.  ↑		

SHOCK-FREE CONFIGURATIONS  
IN  
TWO- AND THREE-DIMENSIONAL TRANSONIC FLOW  
R. SEEBASS  
MRC Symposium on Transonic, Shock  
and Mult-dimensional Flows  
Madison, Wisconsin, May 13-15, 1981

Accession For	
NTIS GRA&I	<input checked="" type="checkbox"/>
DTIC TAB	<input type="checkbox"/>
Unannounced	<input type="checkbox"/>
Justification	
By _____	
Distribution/ _____	
Availability Codes	
Dist	Avail and/or Special
A	



### I. INTRODUCTION.

This paper addresses the rather narrow subject of finding airfoil and wing shapes that are free from shock waves even though the local flow speed exceeds the speed of sound. This research stems directly from an invitation we made to Helmut Sobieczky of the Deutsche Forschungs- und Versuchsanstalt für Luft- und Raumfahrt in Göttingen, West Germany, to spend the academic year 1977-1978 at the University of Arizona. My specific proposal to Sobieczky was that we collaborate on replacing his complicated analog computations of solutions to the hodograph equations by a fast elliptic solver in order to generate shock-free airfoil designs more effectively. The first part of this paper addresses this study. The second part addresses a much more efficient procedure that we now use to the same end. This second method is a result of Sobieczky's brilliant idea of a fictitious gas for finding shock-free airfoils directly in the physical plane.

The aerodynamic efficiency of turbojet-powered aircraft is proportional to the flight Mach number times the lift-to-drag ratio, viz.,  $M_\infty L/D$ . In addition, the amount of return an aircraft provides on the investment in it is proportional to the flight speed, and hence, to the flight Mach number. At supersonic Mach numbers shock waves are always present and give rise to a wave drag that adversely affects the aero-

dynamic efficiency, and they are also the cause of the sonic boom. As Albert George and I showed some time ago [17], the sonic boom has an irreducible minimum for a given aircraft weight and length, and this is large enough to preclude commercial operation of supersonic aircraft over populated areas.

The rapid rise of petroleum prices has driven the cost of fuel rapidly upward and it now comprises more than 50 percent of the direct operating cost of an aircraft. If air transportation is to remain affordable, we must draw on a number of technologies to provide a substantial improvement in the efficiency of transport aircraft. Fortunately, there are a number of technologies that, when combined, should provide a 40 percent improvement in seat-miles per gallon [18]. For a single DC-10 size aircraft, each 1 percent improvement in  $M_\infty L/D$  saves about \$100,000 per year in fuel costs at present prices [9]. Indeed, by the year 2000, we should achieve 90 seat-miles per gallon for intermediate range flights.

One, albeit small, element of this improvement is better aerodynamic efficiency through special airfoil and wing designs that allow flight at supercritical Mach numbers (i.e., subsonic flight Mach number high enough that local regions of the flow are supersonic) without shock-waves. This avoids the drag associated with this shock wave and, more importantly, the boundary-layer separation that occurs if such shock waves become very strong.

This goal was once thought unattainable. In the mid-1950's Morawetz [11] showed that smooth, i.e., continuous, flows with embedded supersonic regions were mathematically isolated from one another. That is, any small change in the Mach number, or any arbitrary change in the airfoil surface embedded in the supersonic region, would result in the appearance of a shock wave in the flow. This led a number of people, including the author, to conclude that such flows would be of no practical interest. Others were more wise. Wind tunnel studies by Pearcey [14], and by Whitcomb [26] showed that such flows did exist and were of practical importance. Subsequent theoretical studies by Nieuwland [13] and Bauer, Garabedian and Korn [1] led to techniques for finding

shock-free airfoil shapes. Boerstoel [2] later improved this technique. Sobieczky [19] developed yet another method that employed a rheo-electric analog computer to solve hodograph-like equations. These earlier contributions are not reviewed here.

The first part of this paper deals with the inverse problem: given an airfoil pressure distribution, find the airfoil that has that pressure distribution. And it also deals with the extension of this procedure to airfoils with an embedded supersonic region. This we call indirect design. The results are a direct consequence of Sobieczky's rheo-electric analog design method where the emphasis was on finding shock-free airfoils. This extension was conceived and used by Sobieczky [20] and further developed by Hassan [5].

The second part of this paper treats Sobieczky's generalization of this process [21]; it provides a tool for the routine design of shock-free airfoils and wings.

## II. INDIRECT DESIGN OF AIRFOILS.

The basic problem we address here is to find an airfoil in two-dimensional, irrotational, flow that has a prescribed pressure distribution. This flow is described by a stream function,  $\psi$ , that guarantees the conservation of mass, that is,

$$\text{curl}(\underline{\psi q}) = \rho \underline{q}$$

so that

$$\text{div}(\rho \underline{q}) = 0,$$

where

$$\rho/\rho_\infty = [1 + \frac{\gamma-1}{2} M_\infty^2 (1 - q^2)]^{1/(\gamma-1)},$$

and the symbols have their usual meanings. Because the flow is irrotational there is a velocity potential,  $\phi$ , such that

$$\underline{q} = \text{grad } \phi.$$

In the direct problem we seek solutions of

$$Q_1 \phi = 0 \tag{1}$$

where

$$\phi_n = 0$$

on the airfoil and  $\phi$  is asymptotic to the potential for a free stream flow past a vortex, of strength equal to the jump in  $\phi$  at the airfoil's trailing edge, located inside the airfoil. Or we may solve a similar equation, viz.,

$$Q_2 \psi = 0 \quad (2)$$

with

$$\psi = 0$$

on the airfoil and with similar asymptotic boundary conditions. Here  $Q_1$  and  $Q_2$  are simple quasi-linear operators of second order. If we interchange the dependent and independent variables in (1) and (2), then we will have linear equations for the coordinates. It is much simpler to introduce the hodograph variables  $q$ , the flow speed, and  $\theta$ , the flow deflection angle as independent variables. This leads to (see, e.g., [25])

$$L_1 \phi = 0 \quad \text{or} \quad L_2 \psi = 0, \quad (3)$$

where  $L_1$  and  $L_2$  are linear, second-order operators. But we do not know the airfoil boundary in the  $q, \theta$ -plane. However, in our approach we wish to specify the pressure, or equivalently  $q$ , and find the airfoil. Figure 1a is a sketch of a supercritical flow past an airfoil that has lift. In this case the hodograph image of the flow will be two-sheeted and appear like that sketched in Figure 1b. Actually, it is mathematically convenient to introduce the variable

$$v = \int_{q^*}^q \sqrt{|1 - M^2|} \frac{dq}{q}$$

in place of  $q$  in equations (3) to reduce equations (3) to their canonical form. For the stream function we have

$$\psi_{vv} \pm \psi_{\theta\theta} - \frac{K'(v)}{K(v)} \psi_v = 0, \quad (4)$$

where  $\pm$  is appropriate if  $M \leq 1$ , and

$$K(v) = \sqrt{|1 - M^2|}/\rho.$$

The subscript  $( )_*$  refers to the sonic state where  $q = a = a_*$  and  $M = 1$ . The variable  $v$  is the usual Prandtl-Meyer function for  $M > 1$ . Sobieczky refers to these variables, viz.,  $v$ ,  $\theta$ , as the rheograph variables because equation (4)

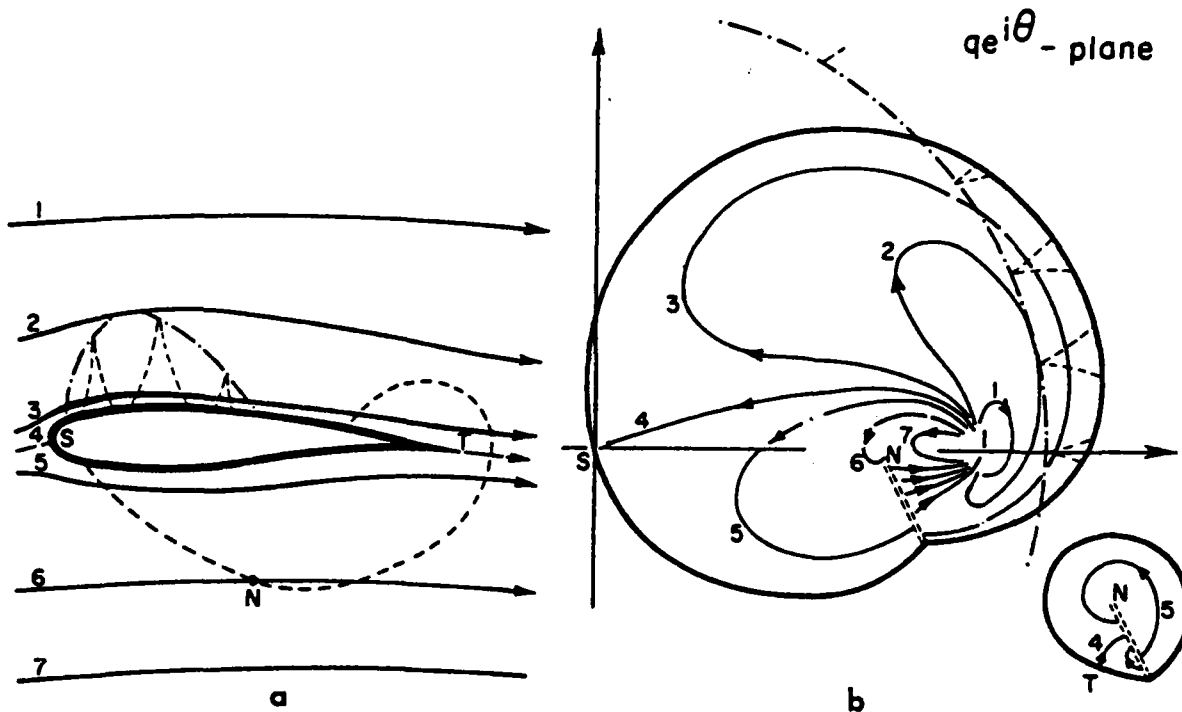


Figure 1. The physical plane (a) and its hodograph image (b).

can be solved by electrostatic means if one supplies a conductor of varying conductivity, as he did by punching holes of varying size in conducting paper. But the general form of equation (4) is invariant under a conformal mapping and we can clearly map the subsonic region of the flow (see Figure 1b) in the  $q, \theta$  or  $v, \omega$  planes into a unit circle. This simple device, suggested by Sobieczky [20], and followed by Hassan [5], provides us with a simple boundary value problem that may be solved efficiently with a fast direct solver. Thus, we map the subsonic portion of Figure 1b into the unit circle of Figure 2 with an unknown mapping of the form

$$\zeta = re^{i\omega} = f(v + i\theta).$$

We insist that this mapping be conformal and hence  $v(r, \omega)$  and  $\theta(r, \omega)$  are harmonic:

$$\nabla^2 v = \nabla^2 \theta = 0.$$

If we give the pressure on the mapped airfoil where the flow is subsonic, then we know  $v$  there. And on the sonic line  $v = 0$ . So  $v$  is known on the unit circle and we can find  $v$  and  $\theta$  to within an arbitrary constant by Fourier series. We must be careful to take into account the behavior of  $v$  as

$q \rightarrow 0$ , viz.,  $v \propto \log q$ . Given the flow conditions at infinity, we know  $v_\infty$ ,  $\theta_\infty$ , and this locates the point at infinity, I. The stream function is singular there, and hence we use the bilinear transformation to map I to the origin of the  $\zeta$  plane

$$\zeta' = r'e^{i\omega'}.$$

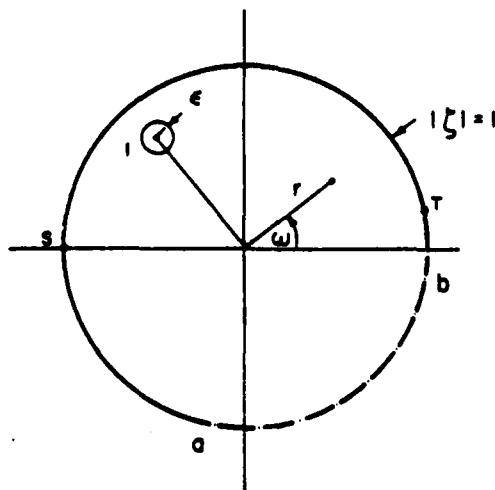
Now on the airfoil boundary  $\psi = 0$  and we may provide a guess for  $\psi(\omega')$  on the sonic line. Thus, we iteratively solve

$$\nabla^2 \psi^n = \left[ \frac{K_r}{K} v_{r'} \psi_{r'}^{n-1} + \frac{K_\omega}{K} v_\omega \left( \frac{1}{r'} \psi_\omega^{n-1} \right) \right],$$

with  $\psi(\epsilon, \omega')$  as  $\epsilon \rightarrow 0$  and  $\psi(1, \omega')$  known, using a fast Poisson solver. Hassan [5] employs the sixth-order solver of Roache [16]. Because on the sonic line  $\psi_{r'}(1, \omega') \approx g(\omega')(1 - r')^{-1/3}$ , Hassan uses the isotach for  $M_\infty = 0.99$  in place of the sonic line and finds the sonic values by Taylor series. The physical plane image of the airfoil and sonic line combination is simply found by integration around the unit circle using (see, e.g., [16])

$$dz = \frac{e^{i\theta(\omega')}}{q(\omega')} [\phi_\omega(1, \omega') - i\psi_{r'}(1, \omega')] d\omega'.$$

This does not necessarily provide a closed airfoil and the input must be adjusted to obtain a satisfactory solution [6]. Now the given pressure distribution is associated with known points on the airfoil and the input pressure distribution may



$\zeta$ -plane

Figure 2. The  $(r, \omega)$  plane image of the subsonic portion of the airfoil surface and the sonic line. See Figure 1.

have to be adjusted to achieve a satisfactory pressure distribution on the airfoil.

For supercritical flows the data on the sonic line is integrated using the method of characteristics to find the airfoil shape consistent with the sonic line data. To be specific,

$$d\phi \mp K(v)d\psi = 0 \quad (5a)$$

on

$$v \mp \theta = \text{const}, \quad (5b)$$

and the sonic line data  $\phi(\theta)$  and  $\psi(\theta)$  are integrated to find the locus  $\psi = 0$ , that is, the airfoil. Now the Jacobian of the map back to the physical plane may vanish before the line  $\psi(v, \theta) = 0$  is reached because  $M > 1$ , in which case a limit

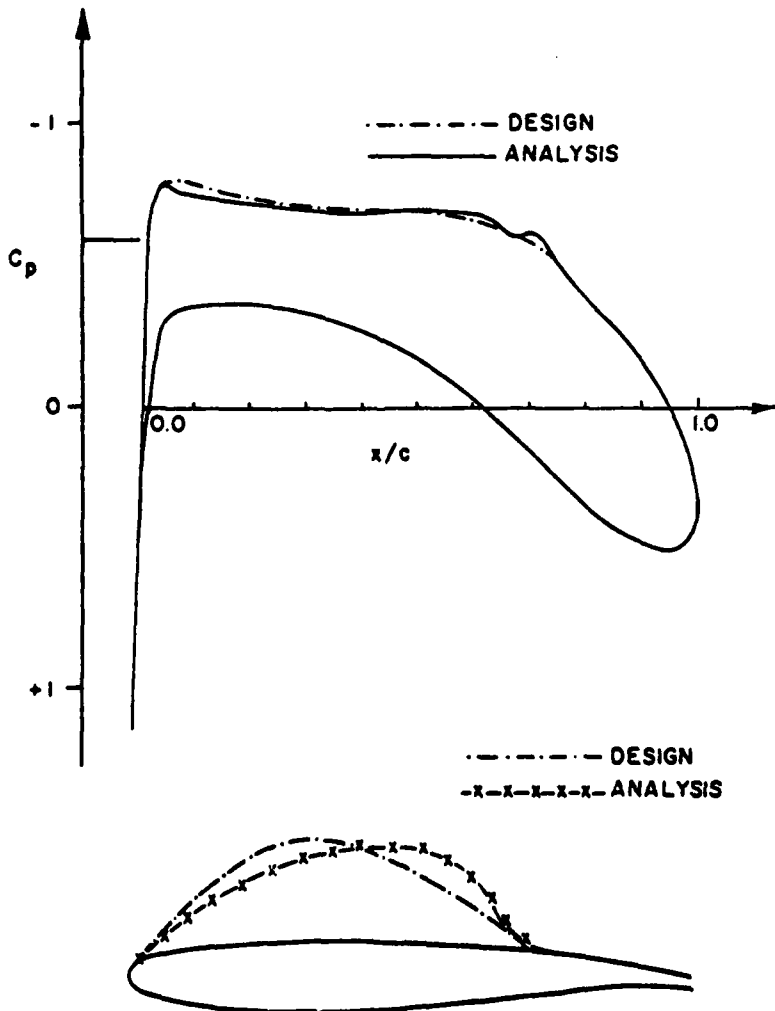


Figure 3. Comparison of the design pressure and sonic line with that computed for the designed airfoil.

line [25] may appear in the physical plane. This means that the sonic line data is not compatible with shock-free flow, and new input data must be given.

One typical result of the process is shown in Figure 3 (from [20]). While this method is effective in finding shock-free airfoils, a more direct procedure for doing so is described in the next section. The main virtues of this procedure are that it is an effective tool for finding subcritical airfoils with desirable pressure distributions, and it led Sobieczky to his clever idea [21, 22] for the nearly direct design of shock-free airfoils and, more importantly, wings.

### III. SHOCK-FREE AIRFOIL DESIGN.

Recall that in the previous section we used a fast Poisson solver iteratively to solve for the subsonic portion of the flow past an airfoil. For supercritical Mach numbers this provided data on the sonic line and the supersonic flow was computed using the method of characteristics. If the sonic line data was inconsistent with shock-free supersonic flow, then the input was modified. Sobieczky [21] observed that this process could be mimicked in the physical plane by changing the equation relating the density to the flow speed when the flow was supersonic in such a way that the governing equation remained elliptic. Thus we solve

$$\operatorname{div}(\rho \nabla \phi) = 0 \quad (6a)$$

where

$$\frac{\rho}{\rho_\infty} = \begin{cases} [1 + \frac{\gamma-1}{2} M_\infty^2 (1 - q^2)]^{1/\gamma-1}, & q \leq a \\ \rho_f / \rho_\infty, & q > a. \end{cases} \quad (6b)$$

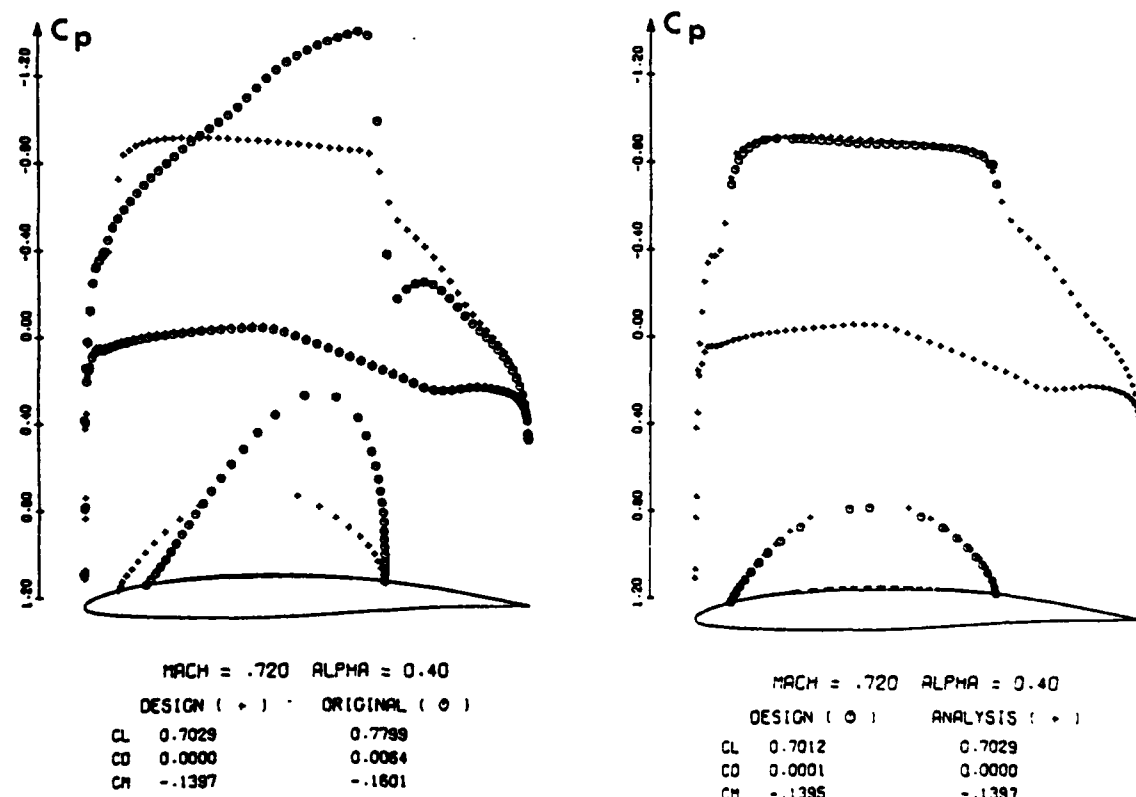
If we wish equation (5) to be elliptic, and we limit our attention to fictitious densities of the form  $\rho_f = \rho_f(q)$ , then we must have

$$\frac{d(\rho_f q)}{dq} > 0.$$

Thus we compute the flow past a baseline airfoil which has been selected on the basis of its subcritical performance. We may wish to alter it slightly in advance of our calculation,

using equation (6) to give it more thickness to compensate for a subsequent reduction in thickness. This fictitious solution satisfies the boundary conditions and the correct equations where  $q < a$ . We take the data, viz.,  $\phi$  and  $\theta$ , that the solution provides on the sonic line and generate  $\psi(\theta)$  from the known relations between  $\phi$  and  $\psi$ . We then recalculate the supersonic domain using equation (5). Of course, if a limit line intervenes we must alter our baseline airfoil, the free stream Mach number, the angle of attack, or the fictitious density relation (6b) and repeat the process.

Figure 4a compares the pressure on an NACA 64A410 airfoil before and after it has been subjected to this design process; it also shows the sonic line (and shock) on the original 64A410 computed using the correct density law, and the sonic line computed using the fictitious density law (6b). The calculation of the supersonic flow by characteristics with the correct density-flow speed relation defines a new



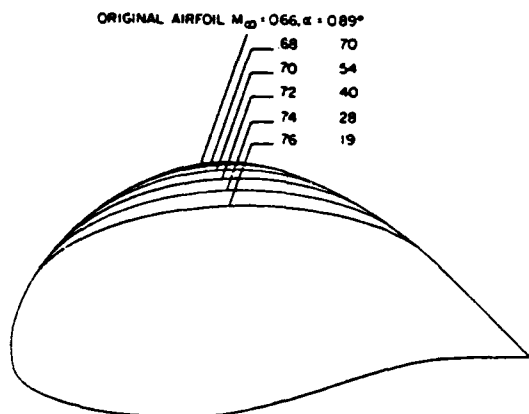
Comparison of the pressure coefficients and sonic lines for the baseline NACA 64A410 and the shock-free airfoil obtained from it by the direct design procedure.

Comparison of the pressure coefficient and the sonic line obtained by the design calculation that modifies the airfoil shape with those obtained by computing the flow past the modified airfoil.

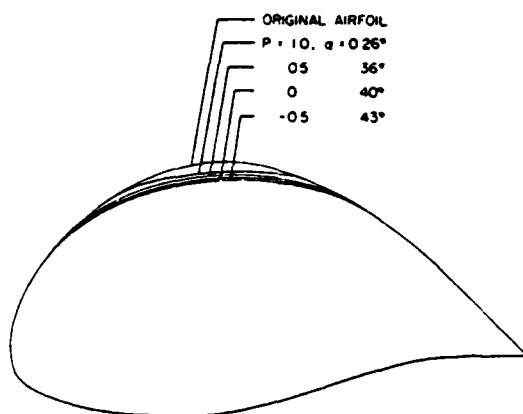
Figure 4. Airfoil designed using the fictitious gas  $\rho_f = \rho_\infty$ .

airfoil shape in the supersonic zone and predicts the indicated pressure on this new shape. A recalculation of the flow past the resulting airfoil is compared with the predicted pressures in Figure 4b. The algorithm used is Jameson's FLO6 [7] which has proved to be very reliable for inviscid flows. Of course the lift coefficient and thickness of the designed airfoil are less than those of the original airfoil. We may find additional designs by fixing the lift coefficient and varying the Mach number, by fixing the Mach number and varying the angle of attack, or by changing the gas law. Frequently we have used

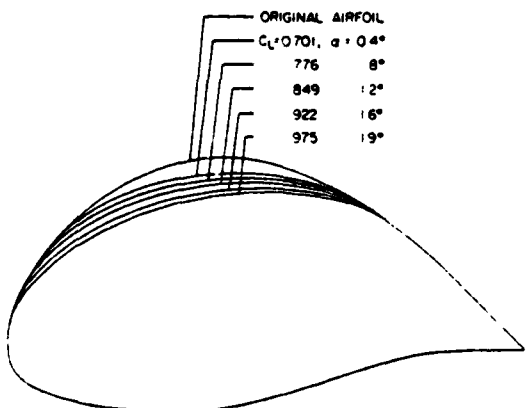
$$\frac{P_f}{P_*} = \left( \frac{a_*}{q} \right)^P \quad (7)$$



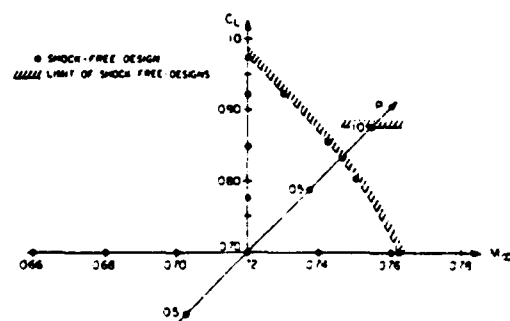
Shock-free airfoil shapes for fixed lift coefficient  $C_L = 0.70$  and varying Mach number. The fictitious gas has a constant density in the supersonic domain ( $P=0$ ). The baseline airfoil is an NACA 64A410.



Shock-free airfoils for fixed Mach number  $M_\infty = 0.72$  and lift coefficient  $C_L = 0.70$ , varying the exponent  $P$  of Eq. (1c) and thus changing the density's dependence on flow speed. The baseline airfoil is an NACA 64A410.



Shock-free airfoil shapes for fixed Mach number  $M_\infty = 0.72$  and varying lift coefficient. The fictitious gas has a constant density in the supersonic domain ( $P=0$ ). The baseline airfoil is an NACA 64A410.



Parameter space explored for the shock-free airfoils that can be obtained when the baseline configuration is an NACA 64A410 airfoil.

Figure 5. Shock-free airfoil shapes for varying  $M_\infty$ ,  $C_L$ , and  $P$ .

where  $P < 1$ . The results of such a study are shown in Figure 5. They indicate the wealth of solutions available by this technique. It also depicts shock-free designs found in  $P$ ,  $C_L, M_\infty$  space.

### IIIa. VISCOUS EFFECTS.

Real flows are of course viscous and even for very large Reynolds numbers we must take the boundary layer displacement effect into account. In the main, such effects are weak and we may calculate the inviscid flow and use its pressure to compute the boundary displacement thickness,  $\delta^*$ .

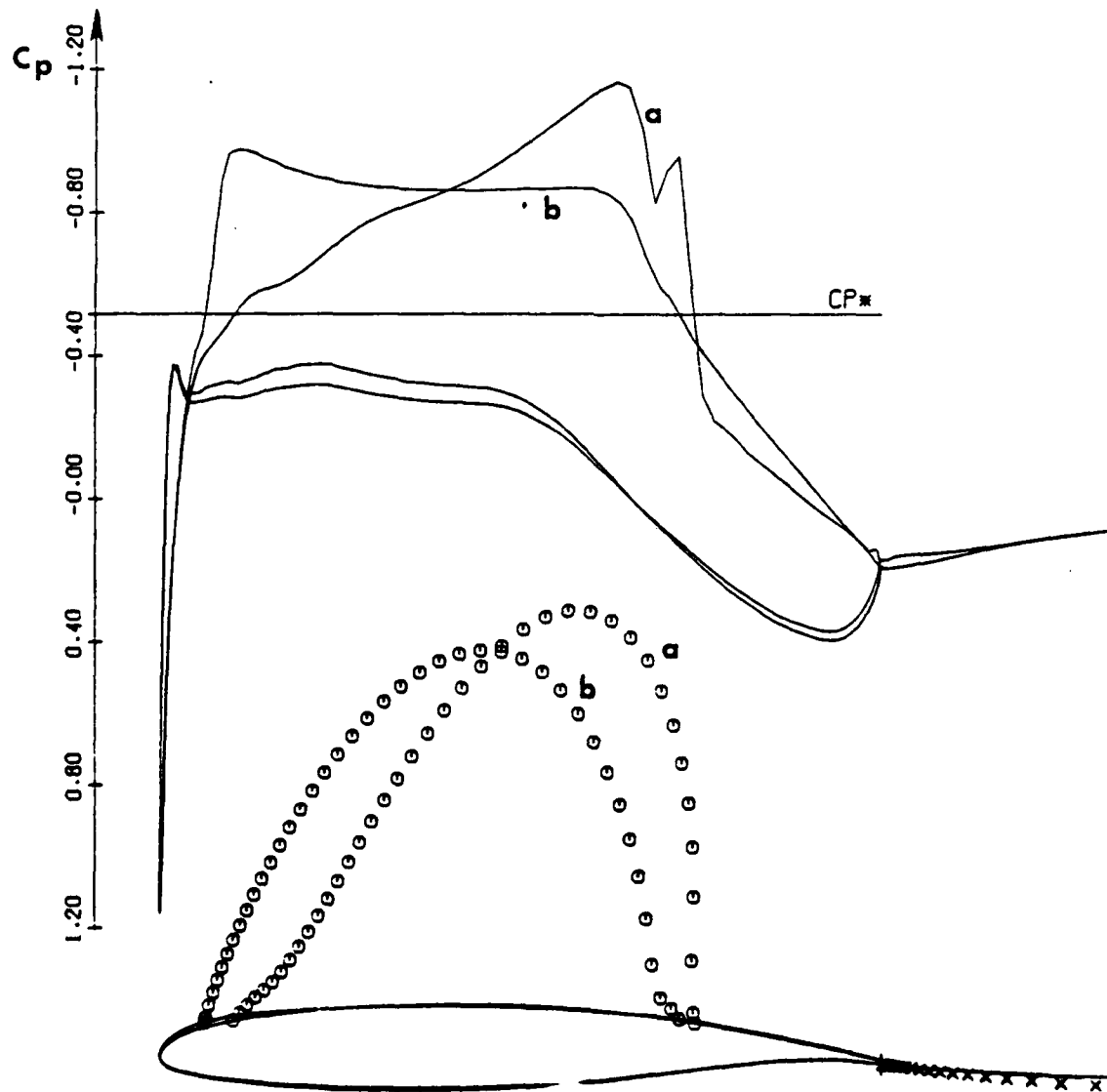


Figure 6. Comparison of  $C_p$ 's and sonic lines for two 11.7% thick airfoils.<sup>19</sup> Airfoil (a) is a thinned GA(W)-2; airfoil (b) is a shock-free design.

There are local, strong inviscid-viscous interactions at the foot of a shock, at the trailing edge, and when the boundary layer separates from the airfoil, and in these regions we must couple the computation of the inviscid flow field with that of the boundary layer. The strong interaction that occurs at the trailing edge has been coupled with Green's lag entrainment model of the integral boundary layer equations by Melnik and his co-workers at Grumman [10] in the Grumfoil algorithm. If we make the not so brash assumption that the boundary layer displacement thickness for a shock-free design will grow in much the same way as it does for the fictitious gas we may try to find shock-free designs in the presence of viscous-inviscid interactions, even when they are strong.

Nebeck [12] has conducted such a study with the Grumfoil algorithm and markedly improved the design of the Va-2 airfoil designed by the German aerospace industry. A subsequent study by Cosentino (private communication) using the GA(W)-2 airfoil provided an 11.7 percent thick airfoil that he estimates to have 73 less counts of drag than an 11.7 percent thick version of the GA(W)-2. His airfoil and the pressure distribution computed using Grumfoil are compared with the thinned GA(W)-2 and its pressure distribution in Figure 6.

#### IV. SHOCK-FREE WING DESIGN.

When this airfoil technology is applied to wings, especially swept wings, the results are not very satisfactory. Indeed, typical results are sketched in Figure 7, which shows that three-dimensional effects will lead to shock waves unless they are explicitly taken into account in the design process. Conceptually, at least, we can imagine the process of Section II extended to three dimensions where we tackle a problem like that sketched in Figure 8a. But we must recall the sketch of Figure 8b. In two dimensions we cannot distinguish the forward facing Mach lines, PA, PC, emanating from point P, from the upward facing Mach lines PC, PB that also originate at P. But once we consider the flow to be three-dimensional, we surely can distinguish the fore Mach cone PAA'C'C from the surface PCC'A'ADD'B'BP. In other words, while we cannot distinguish the time-like direction for

$$-\ddot{\phi}_{xx} + \ddot{\phi}_{yy} = 0,$$

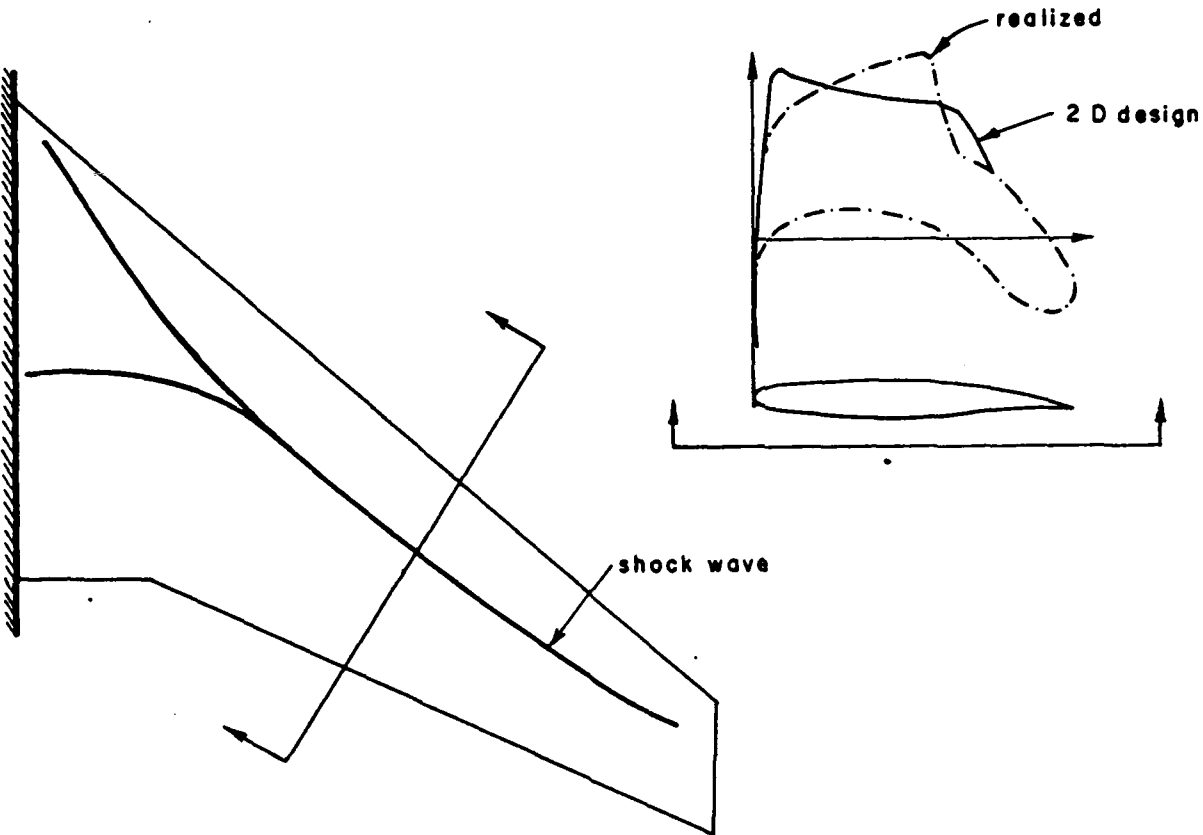
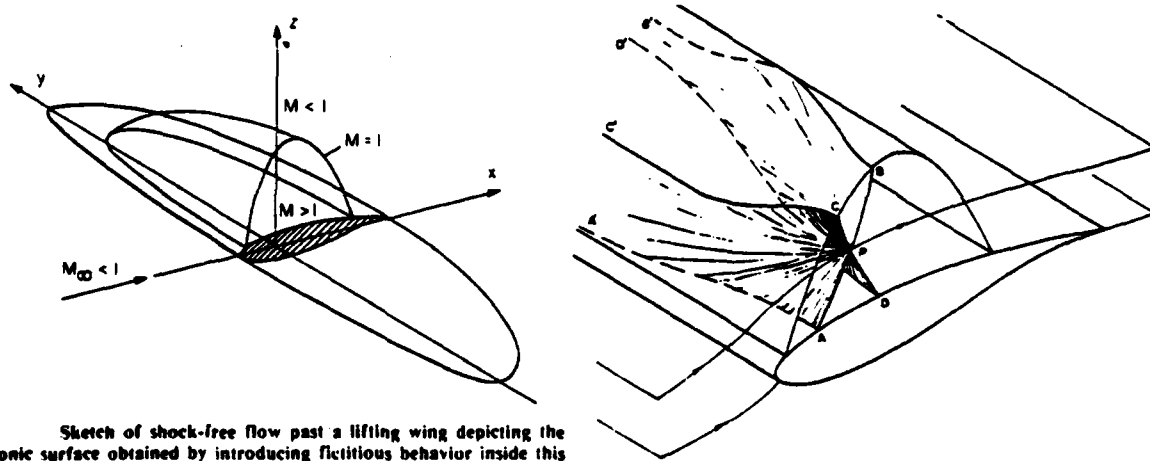


Figure 7. Three-dimensional effects on a wing constructed from shock-free airfoils.



Sketch of shock-free flow past a lifting wing depicting the sonic surface obtained by introducing fictitious behavior inside this surface that results in elliptic equations.

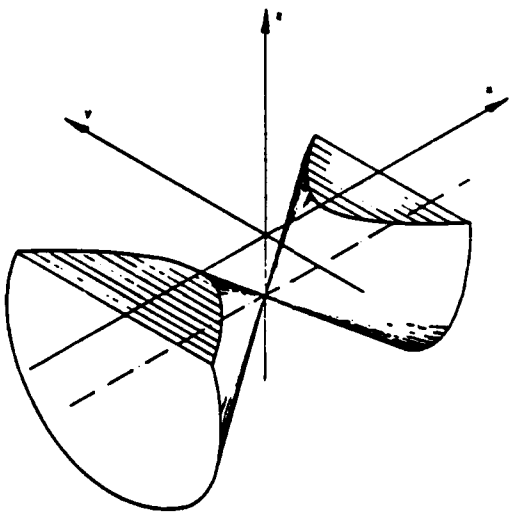
Sketch of Mach conoids for a two-dimensional flow.

Figure 8. Ill-posed boundary-value problem that arises for wings.

clearly only  $x$  is time-like in

$$-\phi_{xx} + \phi_{yy} + \phi_{zz} = 0. \quad (8)$$

When we extend Sobieczky's fictitious gas concept to three dimensions we are essentially trying to solve equation (8) by giving data on the  $x, y$ -plane as sketched in Figure 9, and trying to find the solution for negative  $z$ . This problem is clearly ill-posed. The modal solution to equation (8) is



Mach cones of the linear wave equation and their intersection with the plane where the initial values are given.

Figure 9. Boundary-value problem for equation (8).

$$\phi \propto \exp[i(k_1 x + k_2 y + k_1^2 - k_2^2 z)]$$

and if the wave numbers of interest in the  $y$  direction,  $k_2$ , exceed those of interest in the  $x$  direction,  $k_1$ , the solution will grow exponentially. Indeed, L. E. Payne (private communication) has shown that for any initial data the solution will eventually grow exponentially in  $z$ . But for most practical solutions the wave numbers of interest in the  $x$ , or chordwise, direction are much higher than those in the  $y$ , or spanwise, direction. One can, of course, precondition the initial data to suppress the instability associated with this ill-posed problem, but we have not found this to be necessary.

One of the frequently used algorithms for three-dimensional wings is FLO22, which was developed by Jameson and Caughey [8]. It is a nonconservative code and will not capture shock waves correctly. But for our purpose of shock-free wing design it is perfectly adequate. Here we must introduce a fictitious sound speed rather than a fictitious density. Such sound speed laws and their relation to the fictitious density laws may be found in [4]. We compute the supersonic flow by considering the conservation of mass,

$$(a^2 - u^2)u_x + (a^2 - v^2)v_y + (a^2 - w^2)w_y \\ - 2uvw_x - 2uwv_z = 0$$

and two of the three irrotationality conditions, viz.,

$$w_x - u_z = 0 \quad \text{and} \quad w_y - v_z = 0,$$

as a system of three equations for the vector  $\underline{U}$  = transpose  $(u, v, w)$ , viz.,

$$AU_{-x} + BU_{-y} + CU_{-z} = 0.$$

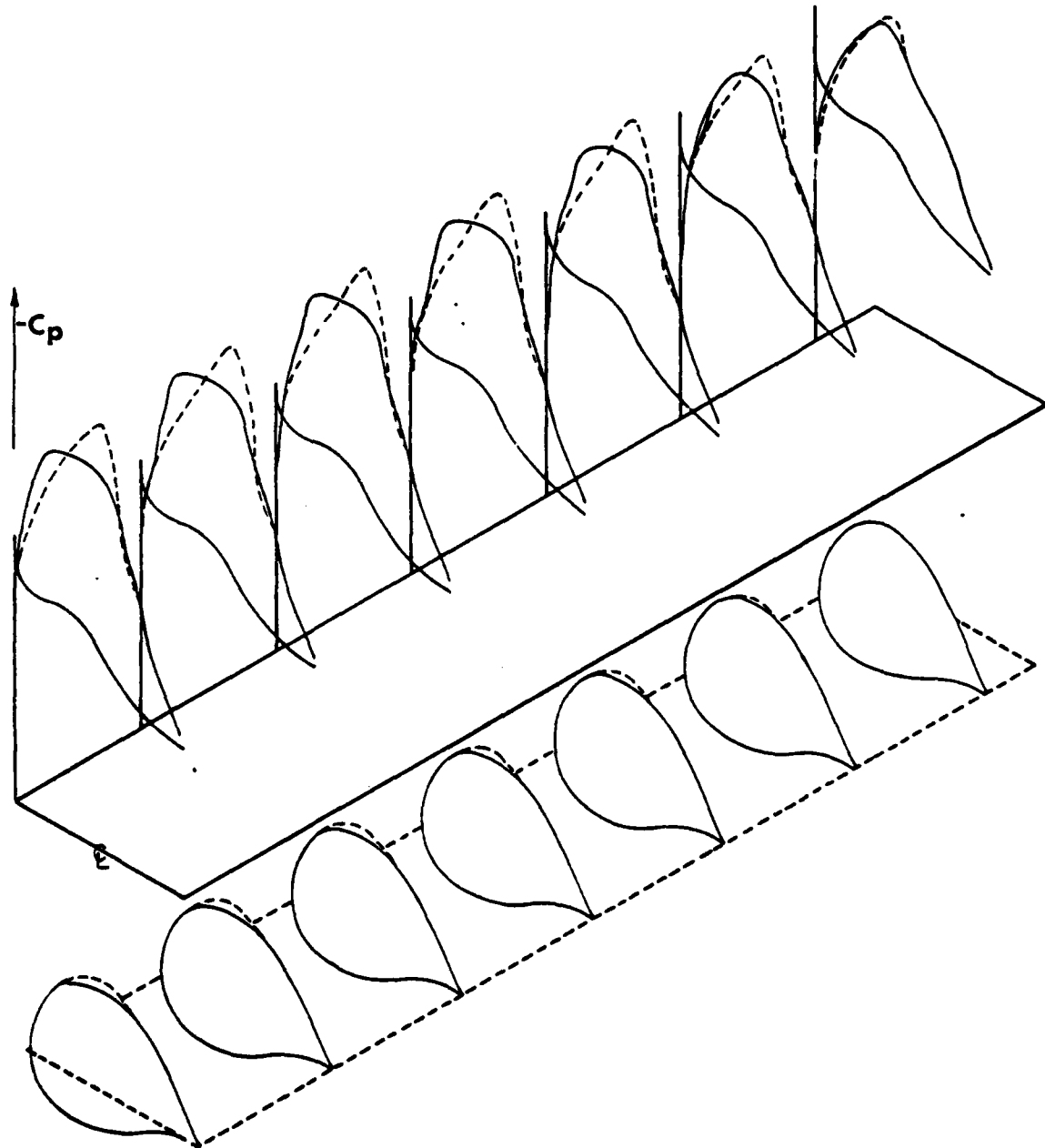


Figure 10. Three-dimensional shock-free flow over a rectangular wing of aspect ratio 10 at  $M_\infty = 0.70$ . The NACA 64A410 airfoil section was used as a baseline for the wing.

We then spline fit the initial data to compute  $\underline{U}_x$  and  $\underline{U}_y$  and find  $\underline{U}_z$  to calculate the data of the next z-level. In general, then, at the  $k^{\text{th}}$ -level

$$\underline{U}_k = \underline{U}_{k-1} - [C^{-1} A \underline{U}_x + C^{-1} B \underline{U}_y]_{k-1/2} \Delta z,$$

where  $[...]$  <sub>$k-1/2$</sub>  indicates a suitable average. Of course  $C^{-1}$  may not exist, indicating the intervention of a limit surface in the supersonic domain. We continue until we find  $\underline{U}$  on the wing surface. For small changes in wing shape a linear, first-order partial differential equation can be solved to find the new wing shape. Further details may be found in [3, 4, 15 and 22]. Yu [27] has also applied this method to wing design using a finite volume code.

Figure 10 shows the results of this design process for a simple rectangular wing with a half-span to chord ratio of 5. The basic wing section was an NACA 64A410. The predicted pressures on the original wing and those on the wing designed to be shock free are the result of the wing section changes indicated below the wing.

#### IVa. VISCOUS EFFECTS.

We have been able to include viscous effects through the Pablim algorithm of C. L. Street (private communication), which couples the three-dimensional boundary layer code of Stock [24] with FLO22. When we compute the flow past the original wing, we use the displacement thickness computed using the shock-free design. This is done to suppress the separation of the boundary layer and favors the original airfoil. We find that the new design, at least at its design point, has an "aerodynamic efficiency" or range factor that typically exceeds a non-shock-free design of the same thickness by 5-15 percent. Such gains are of great practical importance and achieved with minimum effort. A study we have made on improvements to the Learjet Century series aircraft is given in Ref. 3. The GA(W)-2 airfoil used here is probably already superior to the present Learjet airfoil section. Certainly the redesigned wing provides an improvement in supercritical performance and, because it is based on the GA(W)-2 airfoil, should have good low speed performance as well.

## V. THE DESIGN PROCESS.

The design process for shock-free wings must begin with an airfoil and wing planform that provides good low speed and subcritical performance. The art of the designer is in choosing a baseline airfoil and fictitious gas law that will maximize  $M_\infty L/D$  without compromising the established subsonic performance. Here experience is important, as the designer must know what changes in the baseline airfoil and fictitious gas law will produce the desired effects. But current computational tools provide this knowledge at little computational expense. Indeed, an undergraduate student is conducting the investigation of an improved wing for the Learjet Century series aircraft.

## VI. CONCLUSIONS.

While the flows we seek represent mathematically isolated solutions, there is a great wealth of such solutions and they are easy, and inexpensive, to find. Spee [23] has shown that in two dimensions if the local Mach number exceeds  $2/\sqrt{3 - \gamma} = 1.58$  then the flow must be unstable to small unsteady disturbances. Perhaps such shock-free solutions exist with higher local Mach numbers, but we have not found them yet and the condition  $M_\infty = 1.58$  could be a goal the designer should try to achieve. We don't know yet how the drag depends on the flight Mach number at a shock-free design point, nor have we established any theoretical limits on the Mach number, lift coefficient and thickness, beyond which shock-free designs cannot be found. Such theoretical limits could be most useful to the designer.

Let me note in closing that while the ideas fundamental to this investigation are simple, they are mathematically motivated, and they draw upon a wide body of traditional applied mathematics. Also, their implementation depends on computer algorithms carefully constructed to comply with established mathematical principles. And so, it is the author's contention that successful engineering research frequently requires a good appreciation of mathematical principles. And these needs will increase, not decrease, as we rely more and more on computational tools.

#### REFERENCES

1. Bauer, F., P. Garabedian, and D. Korn, Supercritical wing sections III, Lecture Notes in Economics and Mathematical Systems, No. 108, Springer, New York, 1975.
2. Boerstoel, J. W., Design and analysis of a hodograph method for the calculation of supercritical shock-free airfoils, National Aerospace Laboratory, The Netherlands, NLR 77046 U, 1977.
3. Fung, K.-Y., A. R. Seebass, L. J. Dickson, and C. F. Pearson, An effective algorithm for shock-free wing design, AIAA Paper 81-1236, 14th Fluid and Plasma Dynamics Conference, Palo Alto, June 1981.
4. Fung, K.-Y., H. Sobieczky, and R. Seebass, Shock-free wing design, AIAA J., Vol. 18, No. 10, pp. 1153-1158, 1980.
5. Hassan, A. A., Subcritical and supercritical airfoils for a given pressure distribution, Ph.D. Dissertation, University of Arizona, 1981.
6. Hassan, A. A., A. R. Seebass, and H. Sobieczky, Transonic airfoils with a given pressure distribution, AIAA Paper No. 81-1235, AIAA 14th Fluid and Plasma Dynamics Conference, Palo Alto, June 1981.
7. Jameson, A., Iterative solution of transonic flows over airfoils and wings, Comm. Pure and Appl. Math., Vol. 27, pp. 283-309, 1974.
8. Jameson, A. and D. A. Caughey, Numerical calculations of the transonic flow past a swept wing, NASA CR-153297, 1977.
9. Lynch, F. T., Commercial transports - aerodynamic design for cruise performance and efficiency, Douglas Aircraft Company Paper 7026, 1981.
10. Melnik, R. E., Turbulent interactions on airfoils at transonic speeds - recent developments, Computation of Viscous-Inviscid Interactions, AGARD CP No. 291, 1981.
11. Morawetz, C. S., On the non-existence of continuous transonic flows past profiles, I, II, and III, Comm. Pure and Appl. Math., Vols. 9, 10, and 11, pp. 45-68, 107-131, 129-144, 1956, 1957, and 1958.

12. Nebeck, H. E. and A. R. Seebass, Inviscid-viscous interactions in the nearly direct design of shock-free supercritical airfoils, Computation of Viscous-Inviscid Interactions, AGARD CP No. 291, 1981.
13. Nieuwland, G. Y., Transonic potential flow around a family of quasi-elliptical airfoil sections, National Aerospace Laboratory, The Netherlands, TR-T172, 1967.
14. Pearcey, H. H., The aerodynamic design of section shapes for swept wings, Advances in the Aeronautical Sciences, Vol. 13, pp. 277-322, 1962.
15. Raj, P., L. R. Miranda, and A. R. Seebass, A cost-effective method for shock-free supercritical wing design, AIAA Paper 81-0383, AIAA 19th Aerospace Sciences Meeting, St. Louis, January 1981.
16. Roache, P. J., A sixth-order accurate direct solver for the Poisson and Helmholtz equations, AIAA J., Vol. 17, No. 5, pp. 524-526, 1978.
17. Seebass, R. and A. R. George, Sonic-boom minimization, J. Acoust. Soc. Amer., Vol. 51, No. 2, pp. 686-694, 1972.
18. Shevell, R. S., Technological development of transport aircraft, past and future, J. Aircraft, Vol. 17, No. 2, pp. 67-80, 1980.
19. Sobieczky, H., Entwurf überkrittscher Profile mit Hilfe der rheoelektrischen Analogie, Deutsche Forschungs-und Versuchsanstalt für Luft- und Raumfahrt Report DLR-FB 75-43, 1977.
20. Sobieczky, H., Related analytical analog and numerical methods in transonic airfoil design, AIAA Paper 79-1556, AIAA 12th Fluid and Plasma Dynamics Meeting, Williamsburg, July 1979.
21. Sobieczky, H., Die Berechnung lokaler räumlicher Überschallfelder, ZAMM, 58T, 1978.
22. Sobieczky, H., N. J. Yu, K.-Y. Fung, and A. R. Seebass, New method for designing shock-free transonic configurations, AIAA J., Vol. 17, No. 7, pp. 722-729, 1979.
23. Spee, B. M., Investigations on the transonic flow around aerofoils, National Aerospace Laboratory, The Netherlands, NLR TR 69122 U, 1969.

24. Stock, H. W. and H. P. Horton, Ein Integralverfahren zur Berechnung dreidimensionaler, laminarer, kompressibler, adiabater Grenzschichten (to appear in ZFW).
25. von Mises, R., Mathematical Theory of Compressible Fluid Flow, Academic Press, New York, 1958.
26. Whitcomb, R. T. and L. R. Clark, An airfoil shape for effective flight at supercritical Mach numbers, NASA TM X-1109 (confidential), 1965.
27. Yu, N. J., An efficient transonic shock-free wing redesign procedure using a fictitious gas method, AIAA J., Vol. 18, No. 2, pp. 143-148, 1980.

This research was supported by grants from the Air Force Office of Scientific Research, The National Aeronautics and Space Administration, and by the Office of Naval Research. The ideas underlying this research originated with H. Sobieczky. Colleagues K.-Y. Fung and N. J. Yu, as well as graduate students A. Hassan, C. F. Pearson and H. E. Nebeck, are to be credited with their implementation into useful tools. Two undergraduates, G. B. Cosentino and T. F. Schlinkert, respectively, are responsible for some of the design calculations and the computer graphics.

Aerospace and Mechanical Engineering  
University of Arizona  
Tucson, AZ 85721